JYX JYVÄSKYLÄN YLIOPISTO UNIVERSITY OF JYVÄSKYLÄ

This is a self-archived version of an original article. This version may differ from the original in pagination and typographic details.

Author(s): Laulainen, Janne; Kalvas, Taneli; Koivisto, Hannu; Kronholm, Risto; Tarvainen, Olli

Title: Photoelectron emission induced by low temperature hydrogen plasmas

Year: 2018

Version: Published version

Copyright: © AIP Publishing, 2018

Rights: In Copyright

Rights url: http://rightsstatements.org/page/InC/1.0/?language=en

Please cite the original version:

Laulainen, J., Kalvas, T., Koivisto, H., Kronholm, R., & Tarvainen, O. (2018). Photoelectron emission induced by low temperature hydrogen plasmas. In J. Lettry, E. Mahner, B. Marsh, R. Pardo, & R. Scrivens (Eds.), Proceedings of the 17th International Conference on Ion Sources (Article 020001). AIP Publishing. AIP Conference Proceedings, 2011. https://doi.org/10.1063/1.5053243

Photoelectron emission induced by low temperature hydrogen plasmas

Janne Laulainen, Taneli Kalvas, Hannu Koivisto, Risto Kronholm, and Olli Tarvainen

Citation: AIP Conference Proceedings **2011**, 020001 (2018); doi: 10.1063/1.5053243
View online: https://doi.org/10.1063/1.5053243
View Table of Contents: http://aip.scitation.org/toc/apc/2011/1
Published by the American Institute of Physics

Articles you may be interested in

Metal plasma formation in Duhocamis
AIP Conference Proceedings **2011**, 020002 (2018); 10.1063/1.5053244

Towards kinetic models of electron transport in negative ion source presheath
AIP Conference Proceedings **2011**, 020003 (2018); 10.1063/1.5053245

Preface: 17th International Conference on Ion Sources
AIP Conference Proceedings **2011**, 010001 (2018); 10.1063/1.5053241

Preliminary results of 4.0-6.0 GHz extraordinary mode experiments on 2.45 GHz ECRIS
AIP Conference Proceedings **2011**, 020005 (2018); 10.1063/1.5053247

Investigation of laser ablation plasma from thin graphite target
AIP Conference Proceedings **2011**, 020006 (2018); 10.1063/1.5053248

Optical emission spectroscopy for plasma diagnosis of 2.45 GHz ECR ion source at Peking University
AIP Conference Proceedings **2011**, 020004 (2018); 10.1063/1.5053246

AIP | Conference Proceedings

Get 30% off all print proceedings!

Enter Promotion Code PDF30 at checkout

Photoelectron Emission Induced by Low Temperature Hydrogen Plasmas

Janne Laulainen[1,a)], Taneli Kalvas[1], Hannu Koivisto[1], Risto Kronholm[1] and Olli Tarvainen[1]

[1]*University of Jyvaskyla, Department of Physics, Finland*

[a)]Corresponding author: janne.p.laulainen@student.jyu.fi

Abstract. Experimental results of low temperature hydrogen plasma induced photoelectron emission measurements comparing two different plasma heating methods are summarized. By exposing the samples to the vacuum ultraviolet radiation of a filament-driven multi-cusp arc discharge ion source and a 2.45 GHz microwave-driven ion source, it has been measured that the total photoelectron emission from various metal surfaces is on the order of 1 A per kW of plasma heating power, which can be increased by a factor of 2–3.5 with a thin layer of alkali metal. The possible effects of the photoelectrons on the plasma sheath structure are studied with a 1D collisionless model extended to include the contribution of photoelectron emission from the surface.

INTRODUCTION

Low temperature hydrogen plasmas of positive (H^+, H_2^+, D^+) and negative (H^-, D^-) ion sources are strong sources of vacuum ultraviolet (VUV) radiation dissipating up to 30 % of the heating power through VUV emission [1, 2, 3, 4]. Plasma induced photoelectron (PE) emission from metal surfaces is a source of free electrons potentially affecting the ion source plasma properties. We have carried out measurements aiming at quantifying the PE emission induced by low temperature hydrogen plasmas. The fundamental data can be used e.g. for improving numerical simulation models to predict the performances of various kinds of plasma devices.

Intense VUV radiation is emitted by hydrogen plasmas as a consequence of electronic transitions from excited states to lower states of neutral atoms and molecules. Typical VUV emission spectra of hydrogen plasmas are presented in Fig. 1. The Lyman-alpha line at 121.6 nm corresponds to the transition from the first excited state to the ground state of atomic hydrogen. The Werner-band originates from the resonant $C^1\Pi_u \rightarrow X^1\Sigma_g^+$ transitions in the singlet system of the hydrogen molecule, the dominant part of the emission being found at wavelengths shorter than 130 nm. The dominant part of Lyman-band emission originating from $B^1\Sigma_u^+ \rightarrow X^1\Sigma_g^+$ transitions is in the wavelength range of 130–170 nm. The molecular continuum from the $a^3\Sigma_g^+ \rightarrow b^3\Sigma_u^+$ transition of the triplet system is assigned to wavelengths longer than 170 nm. It has been experimentally shown that the PE emission is predominantly induced by VUV emission at wavelengths shorter than 150 nm [5] as indicated by the quantum efficiency of PE emission also plotted in Fig. 1.

This paper summarizes and compares the results of the PE emission measurements performed with a filament-driven multi-cusp arc discharge ion source presented in detail in ref. [5] and with a 2.45 GHz ECR-driven microwave ion source presented in detail in ref. [3]. A major difference between the two plasma heating methods is the resulting electron energy distribution function (EEDF). In arc discharge, the EEDF spans from very low energies up to the energy corresponding to the cathode bias forming a rather uniform distribution [6]. In ECR plasmas, the EEDF is often considered (bi-)Maxwellian [7]. The EEDF influences the VUV emission by affecting the volumetric rates of electronic excitations to singlet and triplet systems of the H_2 molecules and the resulting dissociation degree. Also, the effect of PEs on the plasma sheath structure is evaluated hereafter using a model developed by McAdams et al. [8], which is extended by including the PE current density to the surface emission.

Proceedings of the 17th International Conference on Ion Sources
AIP Conf. Proc. 2011, 020001-1–020001-5; https://doi.org/10.1063/1.5053243
Published by AIP Publishing. 978-0-7354-1727-4/$30.00

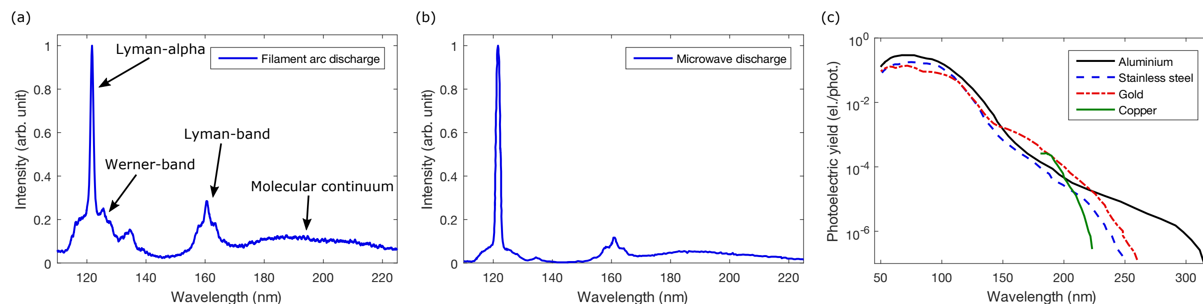

FIGURE 1. (a) Typical VUV emission spectrum of hydrogen plasma of a filament arc discharge (from Ref. [5]) and (b) of a microwave discharge (from Ref. [3]). The spectra are not corrected for spectral transmittance. (c) Photoelectric yield quantum efficiencies for aluminium, stainless steel, gold (from Ref. [9]) and copper (from Ref. [10]).

EXPERIMENTAL METHODS

Hydrogen plasma induced PE emission has been measured from clean (filament and microwave discharges) and cesiated (filament discharge) surfaces of molybdenum, aluminium, copper, tantalum, stainless steel (SAE 304), yttrium, and nickel, using a remote sample illuminated by the plasma light. The measurement setup is presented schematically in Fig. 2. The measurement geometry and conditions are described in detail in Ref. [5]. The distance between the sample and the plasma varied in the two setups, being approximately 1.5 m with the filament source and 0.5 m with the microwave source. Measuring the PE emission directly inside the plasma chamber is not possible, since the measured current would be affected by particle currents from various sources (plasma losses, secondary electron emission, etc.) making it impossible to determine the origin of collected charges. The PE current measured from a remote sample can be considered to give the lower limit for the PE emission inside the plasma chamber, because VUV can be partly absorbed between the sample and the plasma and exposure to VUV and hydrogen plasma can increase the quantum efficiency of the PE emission [10]. The samples, like all the surfaces in ion sources, are technical materials, which are rough in the nanoscale. The sample surface has to be large enough compared to the surface roughness and characteristic dimensions of the variation of different crystal faces etc. in order to measure the average emission. Sample preparation, which included mechanical and chemical cleaning, was performed in atmospheric pressure, and thus the surfaces were covered with their natural oxides and typical vacuum contaminants. The vacuum chamber was evacuated down to 10^{-8} mbar background pressure before introducing 99.9999 % purity hydrogen into the discharge volume. With the remote sample, VUV induced surface aging was observed to change the PE emission slightly.

Monte Carlo methods can be applied to derive an estimate for the total PE current (density), emitted from the walls of the plasma chamber, from the PE current measured with the remote sample. The probability for a single photon to reach the sample surface is calculated and the measured current is divided with the given probability. In the simulation, the light emission profile is assumed homogeneous and isotropic across the plasma chamber volume, which yields the maximum value for the PE emission. In reality, the spatial distribution of the plasma light emission rate depends on the plasma density and temperature profiles. For example, in microwave discharges, the light emission distribution depends on the magnetic field configuration, incident microwave power, and neutral gas pressure [11].

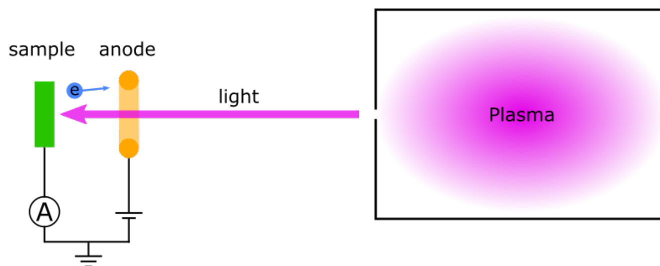

FIGURE 2. Schematic picture of the experimental setup for photoelectron emission measurements.

TABLE 1. Estimated total photoelectron emission. The presented range corresponds to measured PE current variations with different metals (Al, Ta, Mo, Cu, and stainless steel). The current density is determined by scaling the total PE current with the geometry of the particular ion source and, thus, depends directly on the surface area of the plasma chamber.

	PE current ($\mathrm{AkW^{-1}}$)	**PE current density ($\mathrm{AkW^{-1}m^{-2}}$)**
filament arc discharge	0.8–1.2	7–11
microwave discharge	0.9–1.6	20–33

Without accurate information about the density and temperature profiles the total PE emission can only be estimated. It can be argued that the total VUV emission, and hence the PE emission, is most often at least 50 % of the given maximum [2].

EXPERIMENTAL RESULTS

Table 1 summarizes the estimated total PE currents and PE current densities per kW of injected power for filament and microwave discharges. In both cases, the PE current depends linearly on the discharge power. The presented range corresponds to measured PE current variations with different metals, and the current density is directly proportional to the surface area of the plasma chamber. In the case of microwave discharge the estimated total PE emission is slightly higher. The EEDF in the microwave source results to preferential excitation to the triplet states, which leads to higher dissociation rate in comparison to the arc discharge. The volumetric dissociation rate (via $b^3\Sigma_u^+$ state) is calculated to be $2.8–12 \times 10^{16}$ $\mathrm{cm^{-3}s^{-1}}$ for the microwave source [3] and $1.8–4.2 \times 10^{15}$ $\mathrm{cm^{-3}s^{-1}A^{-1}}$ for the filament source [12]. The higher dissociation rate and the subsequent Lyman-alpha emission can explain the higher PE emission observed in the microwave source due to high quantum efficiency at Lyman-alpha wavelength (Fig. 1). The VUV emission spectra measured from both ion sources are presented in Fig. 1, where it can be seen that in the spectrum of the microwave discharge the Lyman-alpha peak is higher than the Werner-band and Lyman-band emissions (relative intensities) in comparison to the filament discharge. It can be assumed, due to the higher power efficiency of the filament source in comparison to the microwave source [2, 3, 12], that the results presented in Table 1 correspond to the minimum difference between the different plasma heating methods.

The effect of alkali metal coverage (Cs and Rb) on the PE emission has been studied with a filament discharge [13]. As an example, Fig. 3 presents the measured PE current from Ta sample during and after Cs deposition. A thin layer of alkali metal increases the PE emission 2–3.5 times in comparison to clean substrate. Emission from thick layer of alkali metal is 60–80 % lower than the emission from clean substrate. Due to the long penetration depth of 10 eV photons in Cs (3.9 µm [14]) in comparison to Ta (8 nm [14]) it is argued that the photons interact predominantly with the Ta substrate even at considerable Cs layer thickness. The work function is lowered by the accumulation of the alkali metal, and thus the PE yield is higher, as long as the emitted electrons are able to propagate through the deposited layer with sufficient energy. The decreasing PE current at thicker layer can be attributed to the short escape depth of the PEs (1-3 nm for few eV electrons [15]) in comparison to the penetration depth of VUV photons. As the Cs deposition is seized the PE current starts to increase again reaching another maximum before saturation. The so

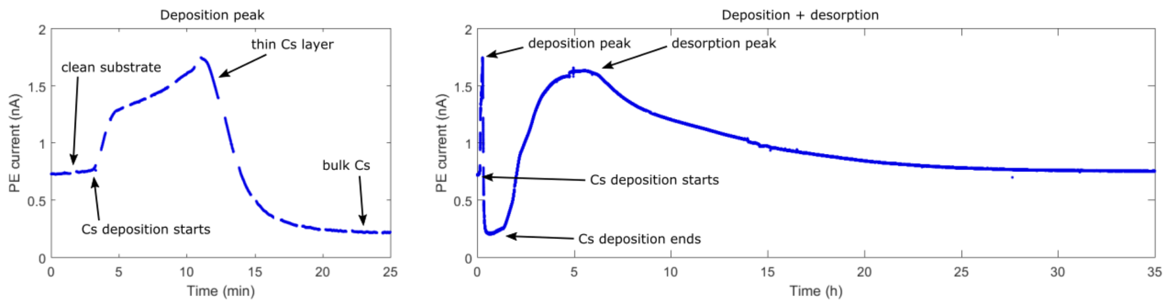

FIGURE 3. Measured photoelectron current from Ta sample with Cs deposition peak shown on the left and both deposition and desorption peaks on the right.

called desorption peak is also observed with photocathodes and is believed to be caused by diffusion and desorption of Cs [16]. In ion sources, the Cs layer is often replenished by constant evaporation. The aim is to sustain a sub-monolayer thickness. However, the minimum measured work function is typically higher than the tabulated values for pure Cs [17].

EXTENSION OF THE SHEATH MODEL

The PE emission may have an impact on the volumetric rates of various plasma processes depending on the intensity and the energy distribution of the emitted electrons. The evaluation of PEs effect on the reaction rates would require the use of a global model. In addition to the plasma chemistry, PE emission can affect the plasma sheath structure, which also determines the final energy of the emitted electrons. A virtual cathode can be formed, if the emission of electrons (and negative ions) from the wall is high enough to prevent the compensation of the space charge by incoming positive ions [8]. If the virtual cathode exists, it limits the transport of surface produced negative ions and the emitted PEs into the plasma depending on their energies. If the PE emission increases the depth of the virtual cathode, it can be considered as a potential limitation for the surface production of negative ions.

PEs effect on the plasma sheath structure is predicted using a one-dimensional analytical model of the sheath in a negative ion source [8]. The collisionless model does not take into account the magnetic field. The model is modified to include PE emission from the wall by substituting the H^- current density j_{H^-} with effective current density

$$j_{eff} = j_{H^-} + \int_0^{h\nu-\phi} j_{PE}(E_{PE}) \sqrt{\frac{m_e}{m_{H^-}}} \sqrt{\frac{E_{H^-}}{E_{PE}}} \, dE_{PE}, \tag{1}$$

where j_{PE} is the PE current density, m_e electron mass, m_{H^-} negative hydrogen ion mass, E_{PE} PE energy, and E_{H^-} negative hydrogen ion energy. A uniform energy distribution ranging from zero to the maximum energy, which corresponds to the difference between the energy of the absorbed photon $h\nu$ and the surface work function ϕ, is used for PEs with $h\nu = 10$ eV and $\phi = 2$ eV corresponding to approximate work function of a cesiated surface. The actual energy distribution of the emitted electrons is unknown. The measured PE current corresponds to the total emission caused by wide range of photon energies. The energy of the emitted electrons also depends on the photon interaction with electrons deeper (than the Fermi level) in the conduction band and on the processes taking place within the material after the actual photon–electron interaction. The measured VUV spectra (e.g. in Fig. 1) together with the quantum efficiencies reported in the literature cannot be used to derive the interaction probability nor the PE energy distribution, because the spectra are not calibrated for spectral response. Thus, an approximation, such as a uniform distribution, must be used. Following Ref. [8] a constant energy of 0.7 eV is assumed for surface produced negative hydrogen ions and the plasma density, electron temperature and positive ion temperature are set to 3.5×10^{17} m^{-3}, 2 eV and 0.8 eV, respectively. It is assumed that there are no volume produced negative ions.

The potential difference between the emitting surface and the plasma, referred as the cathode potential, plays a major role in the significance of the PE emission on the sheath properties. In Fig. 4 the plasma sheath potential is plotted for different cathode potentials with various emission currents. The black line shows the sheath structure at the threshold H^- emission current density creating a virtual cathode. The red line presents the sheath structure with PE current density needed (in addition to H^- current density) for the depth of the virtual cathode to reach 10 % of

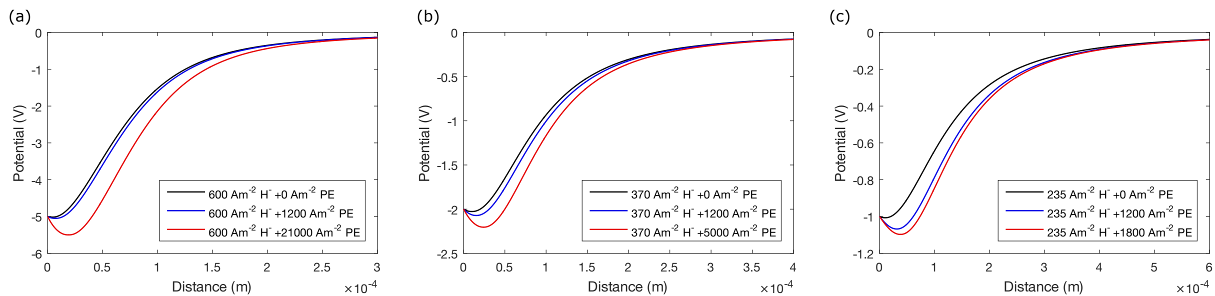

FIGURE 4. Sheath potentials for various H^- and photoelectron emission current densities with cathode potentials of (a) −5 V (b) −2 V (c) −1 V.

the cathode potential. The blue line presents the sheath structure with a constant PE current density of 1200 Am^{-2} demonstrating that the PE emission has a more significant impact on the sheath structure with lower cathode potentials. In H^- ion sources, the plasma electrode is usually biased positively, resulting in decreased potential difference between the plasma and the electrode, in order to reduce the co-extracted electron current [18], which presumably affects the significance of the PE emission.

Are the PE current densities in Fig. 4 realistic? The experimental results suggest that the total PE current from cesiated plasma chamber walls could be as high as 3.5 A per kW of discharge power. For example, in a surface production ion source used for neutral beam injection (ELISE), the plasma is heated with the maximum RF power of 360 kW and the illuminated plasma grid area is 0.9 m^2 [18]. Direct extrapolation from 3.5 AkW^{-1} yields a total PE current density of 140–420 Am^{-2}, if 10–30 % of the emitted light is incident on the grid. On the other hand, the corresponding estimate for a Penning type ion source with up to 3.85 kW of discharge power dissipated in < 1 cm^3 sized plasma contained in a chamber with a surface area of 2.48×10^{-4} m^2 [19], yields a PE current density of 54 kAm^{-2}. In the ion sources used for the PE emission measurements, the light emission depends linearly on discharge power. However, this cannot automatically be assumed to hold for high power ion sources. The realization of a PE emission density needed for a significant influence on the plasma sheath structure depends on the mechanical design of the plasma device, plasma heating method and the discharge power. It can be concluded, that if the order of magnitude for the PE current density reaches 1 kAm^{-2} and the cathode potential is low, the PE emission can be significant for the plasma sheath structure.

ACKNOWLEDGMENTS

This work has been supported by the Academy of Finland under the Finnish Centre of Excellence Programme 2012–2017 (Nuclear and Accelerator Based Physics Research at JYFL) and European Union's Horizon 2020 research and innovation programme under grant agreement No. 654002.

REFERENCES

[1] J. Komppula and O. Tarvainen, Phys. Plasmas **22**, p. 103516 (2015).
[2] J. Komppula, O. Tarvainen, S. Lätti, T. Kalvas, H. Koivisto, V. Toivanen, and P. Myllyperkiö, AIP Conf. Proc. **1515**, p. 66 (2013).
[3] J. Komppula, O. Tarvainen, T. Kalvas, H. Koivisto, R. Kronholm, J. Laulainen, and P. Myllyperkiö, J. Phys. D: Appl. Phys. **48**, p. 365201 (2015).
[4] U. Fantz, S. Briefi, D. Rauner, and D. Wünderlich, Plasma Sources Sci. Technol. **25**, p. 045006 (2016).
[5] J. Laulainen, T. Kalvas, H. Koivisto, J. Komppula, and O. Tarvainen, AIP Conf. Proc. **1655**, p. 020007 (2015).
[6] J. Bretagne, G. Delouya, C. Gorse, M. Capitelli, and M. Bacal, J. Phys. D: Appl. Phys. **18**, p. 811 (1985).
[7] V. A. Godyak, IEEE Trans. Plasma Sci. **34**, p. 755 (2006).
[8] R. McAdams, A. J. T. Holmes, D. B. King, and E. Surrey, Plasma Sources Sci. Technol. **20**, p. 035023 (2011).
[9] B. Feuerbacher and B. Fitton, J. Appl. Phys. **43**, p. 1563 (1972).
[10] D. H. Dowell, F. K. King, R. E. Kirby, J. F. Schmerge, and J. M. Smedley, Phys. Rev. ST AB **9**, p. 063502 (2006).
[11] O. D. Cortázar, A. Megía-Macías, A. Vizcaíno-de Julián, O. Tarvainen, J. Komppula, and H. Koivisto, Rev. Sci. Instrum. **85**, p. 02A902 (2014).
[12] J. Komppula and O. Tarvainen, Plasma Sources Sci. Technol. **24**, p. 045008 (2015).
[13] J. Laulainen, S. Aleiferis, T. Kalvas, H. Koivisto, R. Kronholm, and O. Tarvainen, Phys. Plasmas **24**, p. 103502 (2017).
[14] B. L. Henke, E. M. Gullikson, and J. C. Davis, At. Data Nucl. Data Tables **54**, p. 181 (1993).
[15] M. P. Seah and W. A. Dench, Surf. Interface Anal. **1**, p. 2 (1979).
[16] E. J. Montgomery, "Characterization of quantum efficiency and robustness of cesium-based photocathodes," Ph.D. thesis, University of Maryland, College Park, Maryland, USA. 2009.
[17] R. Friedl and U. Fantz, AIP Conf. Proc. **1655**, p. 020004 (2015).
[18] U. Fantz, P. Franzen, B. Heinemann, and D. Wünderlich, Rev. Sci. Instrum. **85**, p. 02B305 (2014).
[19] D. C. Faircloth and S. Lawrie, private communication (2013).